Using Machine Learning for wall functions including pressure gradients

Lars Davidson

LESisMORE, Kickoff, Sept 2024

Download paper and Python scripts

- Machine learning (ML) is often a method where known data are used for teaching the algorithm to classify a set of data.

- Machine learning (ML) is often a method where known data are used for teaching the algorithm to classify a set of data.
    - Photographs where the machine learning algorithm should recognize, e.g., traffic lights [11].

- Machine learning (ML) is often a method where known data are used for teaching the algorithm to classify a set of data.
  - Photographs where the machine learning algorithm should recognize, e.g., traffic lights [11].
  - ECG signals where the machine learning algorithm should recognize certain unhealthy conditions of the heart [9].

- Machine learning (ML) is often a method where known data are used for teaching the algorithm to classify a set of data.
  - Photographs where the machine learning algorithm should recognize, e.g., traffic lights [11].
  - ECG signals where the machine learning algorithm should recognize certain unhealthy conditions of the heart [9].
  - Detecting fraud for credit card payments [10].

- Machine learning (ML) is often a method where known data are used for teaching the algorithm to classify a set of data.
    - Photographs where the machine learning algorithm should recognize, e.g., traffic lights [11].
    - ECG signals where the machine learning algorithm should recognize certain unhealthy conditions of the heart [9].
    - Detecting fraud for credit card payments [10].
- In my case, input and output are numerical values.

- Machine learning (ML) is often a method where known data are used for teaching the algorithm to classify a set of data.
  - Photographs where the machine learning algorithm should recognize, e.g., traffic lights [11].
  - ECG signals where the machine learning algorithm should recognize certain unhealthy conditions of the heart [9].
  - Detecting fraud for credit card payments [10].
- In my case, input and output are numerical values.
- The ML will then be some form of regression method.

Initial Work [6]

- Machine Learning (`svr`) wall functions were developed
- Good results for channel flow placing the wall-adjacent cell at different locations
- Good results for developing boundary layer flow
- Training the `svr` with steady or instantaneous data: same results
- Training nearest neighbor (Python's `scipy.spatial.KDTree`) with instantaneous data: same results

- **KDTree** will be used for finding y^+.
- It is essentially a fast look-up table
- There will be two sets of data points.
  - One is the target data set, i.e. low-Re IDDES ($\mathbf{X} = [U^+_{target}, y^+_{target}]$)
  - The other one is the wall-function IDDES ($\mathbf{x} = [U^+_{CFD}, y^+_{CFD}]$
- **KDTree** computes the distance between the vectors as

$$\mathbf{d_s} = \mathbf{X}_i - \mathbf{x}_j \tag{1}$$

for all samples i and j and finds the k nearest neighbors for each j.

The Numerical Method

The Numerical Method

- The Python finite volume code pyCALC-LES [5] is used.

- The Python finite volume code pyCALC-LES [5] is used.
- Fully vectorized (i.e. no `for` loops).

- The Python finite volume code pyCALC-LES [5] is used.
- Fully vectorized (i.e. no `for` loops).
- Fractional step. For velocities, second-order central differencing in space and Crank-Nicolson in time.

The Numerical Method

- The Python finite volume code pyCALC-LES [5] is used.
- Fully vectorized (i.e. no `for` loops).
- Fractional step. For velocities, second-order central differencing in space and Crank-Nicolson in time.
- For k and ε, hybrid central/upwind scheme

- The Python finite volume code pyCALC-LES [5] is used.
- Fully vectorized (i.e. no `for` loops).
- Fractional step. For velocities, second-order central differencing in space and Crank-Nicolson in time.
- For k and ε, hybrid central/upwind scheme
- The discretized equations are solved with Python sparse matrix solvers.

- The Python finite volume code pyCALC-LES [5] is used.
- Fully vectorized (i.e. no `for` loops).
- Fractional step. For velocities, second-order central differencing in space and Crank-Nicolson in time.
- For k and ε, hybrid central/upwind scheme
- The discretized equations are solved with Python sparse matrix solvers.
- It runs either on the CPU or the GPU (the GPU is up to 70 times faster)

- The Python finite volume code pyCALC-LES [5] is used.
- Fully vectorized (i.e. no `for` loops).
- Fractional step. For velocities, second-order central differencing in space and Crank-Nicolson in time.
- For k and ε, hybrid central/upwind scheme
- The discretized equations are solved with Python sparse matrix solvers.
- It runs either on the CPU or the GPU (the GPU is up to 70 times faster)
- On the GPU, the Algebraic Multigrid solver in AMGX is used; it very fast.

The Numerical Method

- The Python finite volume code pyCALC-LES [5] is used.
- Fully vectorized (i.e. no `for` loops).
- Fractional step. For velocities, second-order central differencing in space and Crank-Nicolson in time.
- For k and ε, hybrid central/upwind scheme
- The discretized equations are solved with Python sparse matrix solvers.
- It runs either on the CPU or the GPU (the GPU is up to 70 times faster)
- On the GPU, the Algebraic Multigrid solver in AMGX is used; it very fast.
- `cupy` is used to switch from CPU to GPU (`import cupy`)

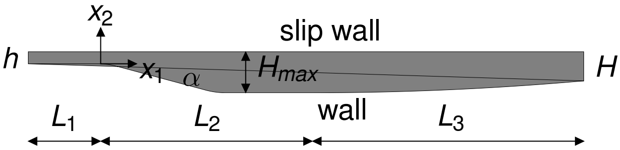

Geometry.

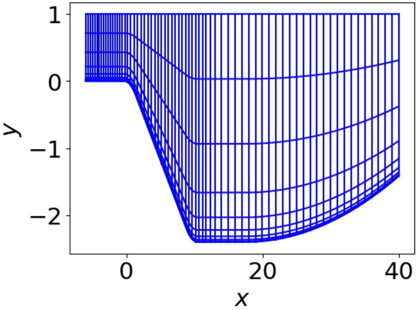

Grid, $x - y$ plane (not to scale). 700×90 cells. Every 10^{th} grid line is shown.

Diffuser, $\alpha = 15^o$.

- $700 \times 90 \times 96$. $k - \varepsilon$ IDDES.
- Inlet b.c. from pre-cursor IDDES channel flow at $Re_\tau = 5\,200$.

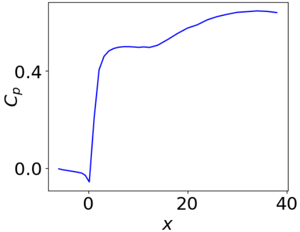

Pressure coefficient.

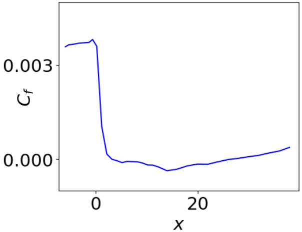

Skin friction.

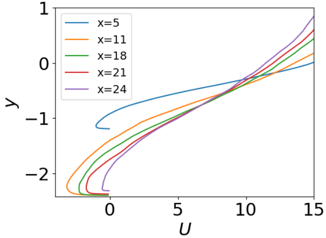

Velocity.

*

Diffuser flow. Target data base.

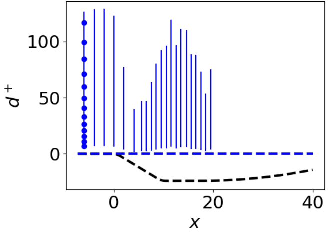

Data points of y^+ vs. x.

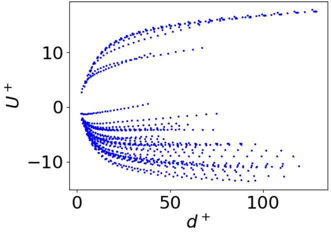

Scatter plot of U^+ and y^+.

Diffuser flow. The target database consists of time-averaged 41 profiles of U^+ vs. y^+ with 26 points in each profile. d the is wall distance. Every second x line and y point are shown.

y_P^+	:	inlet and outlet parameter
U^+	:	inlet and output parameter
u_τ	:	$y_P^+\nu/y_P$

$$
\begin{aligned}
y_P^+ &\quad : \quad \text{inlet and outlet parameter} \\
U^+ &\quad : \quad \text{inlet and output parameter} \\
u_\tau &\quad : \quad y_P^+ \nu / y_P
\end{aligned}
$$

$$
\begin{aligned}
\rho u_\tau^2 &\quad : \quad \bar{u} \text{ equation} \\
C_\mu^{-1/2} u_\tau^2 &\quad : \quad k \text{ equation} \\
\frac{u_\tau^3}{\kappa y} &\quad : \quad \varepsilon \text{ equation}
\end{aligned}
$$

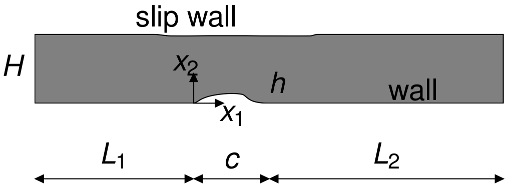

$h = 0.128$. $H = 0.909$, $L_1 = 2.1$, $c = 1$, $L_2 = 4.1$.

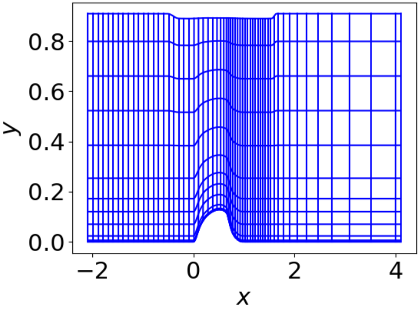

Grid. $582 \times 128 \times 64$ cells. Every 10^{th}.

Hump flow.

TARGET DATABASE 2: RESULTS

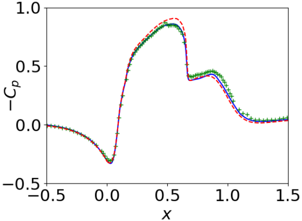

Pressure coefficient.

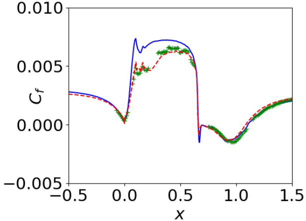

Friction coefficient.

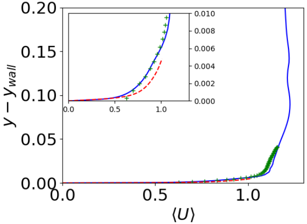

Velocity at $x = 0.65$.

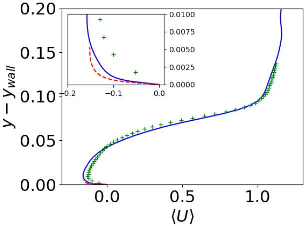

Velocity at $x = 0.80$.

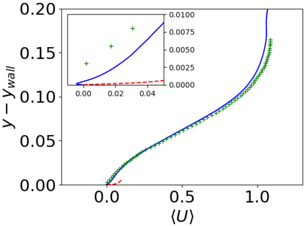

Velocity at $x = 1.10$.

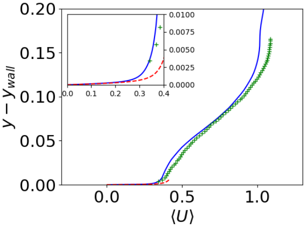

Velocity at $x = 1.30$.

Hump flow, low-Re IDDES. +: experiments [8, 7].

TARGET DATABASE FOR KDTREE . BASELINE: $K = 1$ (ONE NBR).

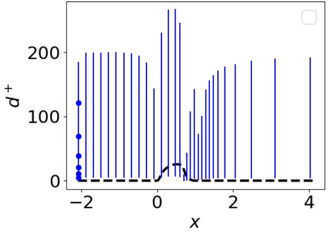

Data points of y^+ vs. x.

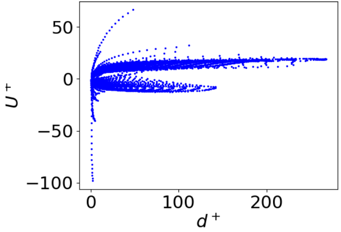

Scatter plot of U^+ and y^+.

Hump flow. d is the wall distance. The target database consists of time-averaged 582 profiles (all grid lines) of U^+ vs. y^+ with 24 points in each profile. Every 20^{th} x line and every 4^{th} y point are shown.

New Wall Function Grid Strategy

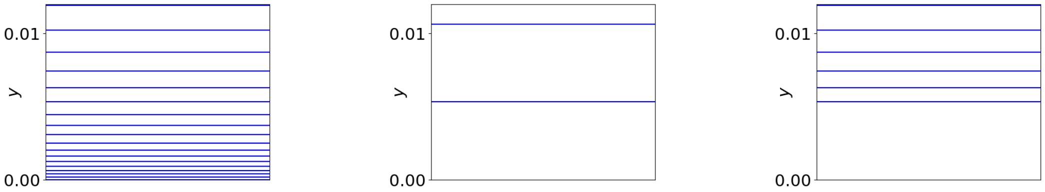

Low-Re number grid. Wall function grid. New wall function grid.

Different grids. —— : grid lines.

- Wall functions based on **KDTree** or Reichardt wall functions
- Wall functions based Reichardt's law

$$\frac{\bar{u}_P}{u_\tau} \equiv U^+ = \frac{1}{\kappa}\ln(1-0.4y^+) + 7.8\left[1-\exp\left(-y^+/11\right) - (y^+/11)\exp\left(-y^+/3\right)\right]$$

  is solved using the Newton-Raphson method `scipy.optimize.newton` in Python.
- Turbulence model: IDDES based on the AKN low-Re $k-\varepsilon$ model
- Instantaneous inlet b.c. from pre-cursor channel IDDES using **KDTree** wall functions
- Grid: $462 \times 70 \times 48$ (low-Re IDDES grid: $600 \times 90 \times 96$)

RESULTS, DIFFUSER FLOW, $\alpha = 15^o$

- $468 \times 70 \times 48$ cells (every 2^{nd} in x and z)

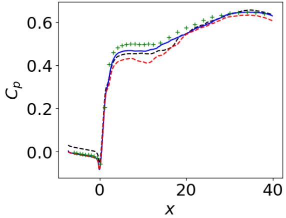

Pressure coefficient.

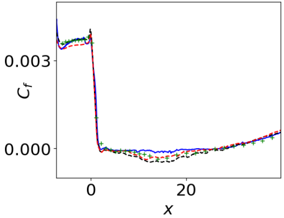

Skin coefficient.

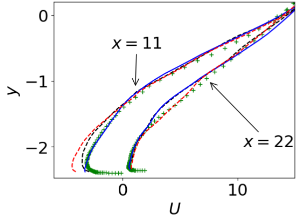

Velocity profiles.

Diffuser flow, $\alpha = 15^o$. —— : **KDTree** using hump flow data; - - - : **KDTree** using diffuser flow data; – – : Reichardt's law; +: low-Re IDDES.

- $387 \times 70 \times 48$ cells (every 2^{nd} in x and z)

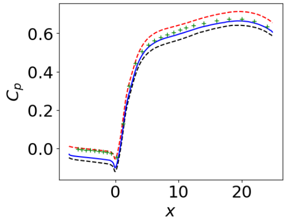

Pressure coefficient.

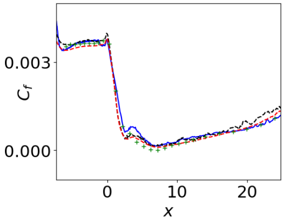

Skin coefficient.

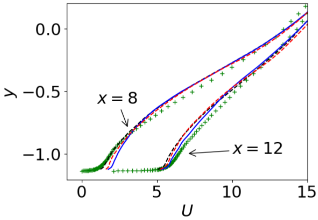

Velocity profiles.

Diffuser flow, $\alpha = 10^o$. —— : **KDTree** using hump flow data; - - - : **KDTree** using diffuser flow data; – – : Reichardt's law; $+$: low-Re IDDES.

- The Reynolds number is $Re_c = 936\,000$. Spanwise extent is $z_{max} = 0.2$.
- The mesh has $291 \times 106 \times 64/32$ cells [x, y, z] (low-Re IDDES $582 \times 106 \times 64$)
- Inlet b.c.
  - Mean from 2D RANS
  - Inlet turbulence: fluctuation from STG
  - Inlet k and ε: 2D RANS plus commutation term in k eq. [3, 1] (Model 3)
- Comparison with
  - Experiments [8, 7]

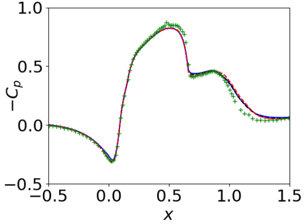

Pressure coefficient.

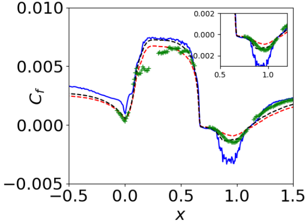

Friction coefficient.

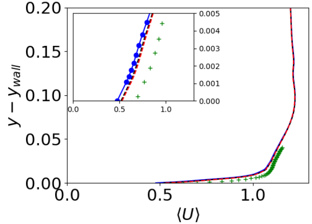

$x = 0.65.$

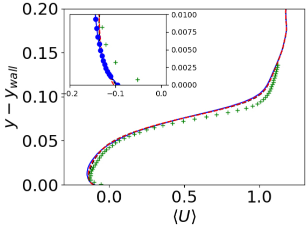

$x = 0.80.$

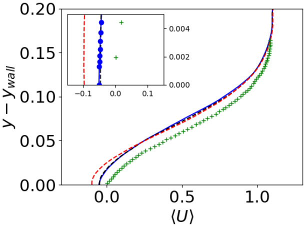

$x = 1.10.$

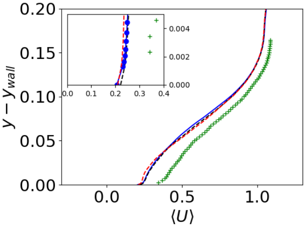

$x = 1.30.$

: **KDTree** hump data; - - - : **KDTree** diffuser data; - - : Reichardt's law; +: exp.

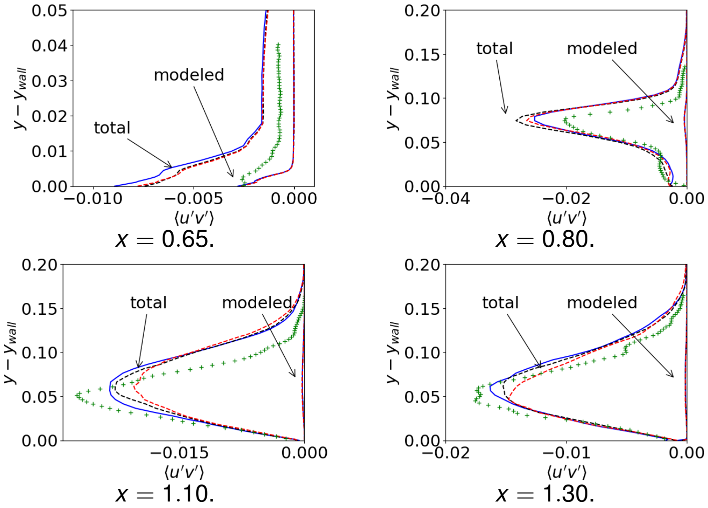

: **KDTree** hump data; - - - : **KDTree** diffuser data; – – : Reichardt's law; +: exp.

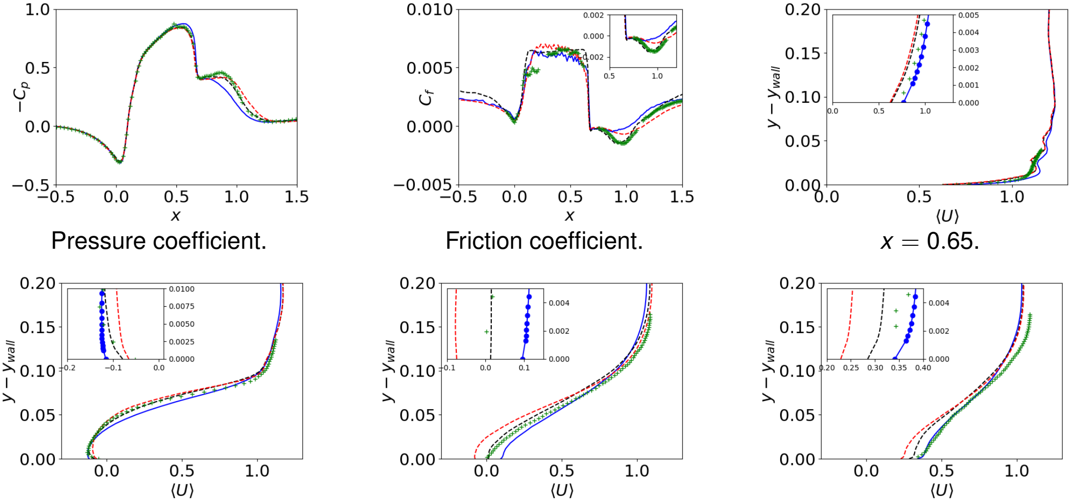

Pressure coefficient. Friction coefficient. $x = 0.65$.

$x = 0.80$. $x = 1.10$. $x = 1.30$.

KDTree hump data; - - - : **KDTree** diffuser data; — — : Reichardt's law; +: exp.

RESULTS, HUMP FLOW. 291 × 106 × 32 CELLS. SHEAR STRESSES

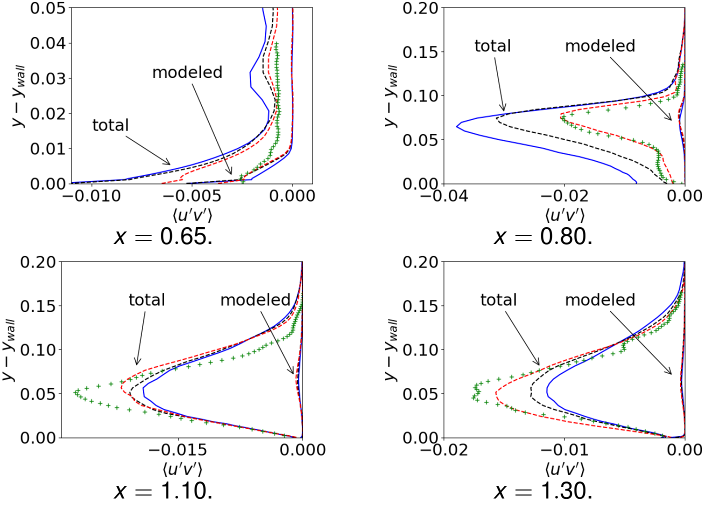

: **KDTree** hump data; - - - : **KDTree** diffuser data; − − : Reichardt's law; +: exp.

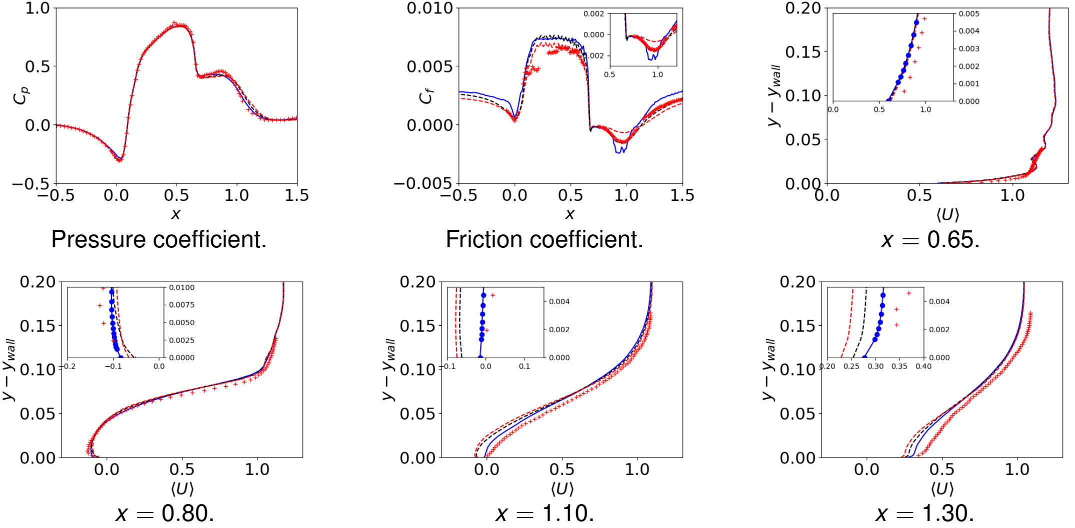

Pressure coefficient. Friction coefficient. $x = 0.65$.

$x = 0.80$. $x = 1.10$. $x = 1.30$.

: **KDTree** hump data; - - - : **KDTree** diffuser data; — — : Reichardt's law; +: exp.

HUMP FLOW. $291 \times 106 \times 32$ CELLS. SHEAR STRESSES, $K = 5$.

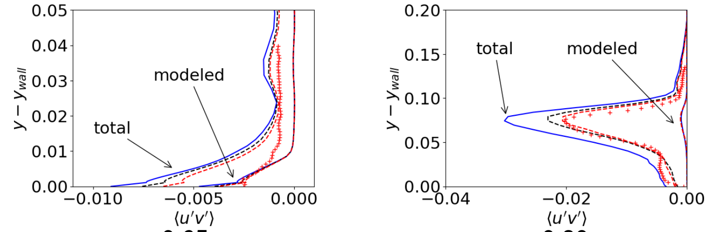

$x = 0.65$. $x = 0.80$.

$x = 1.10$. $x = 1.30$.

—— : **KDTree** hump data; - - - : **KDTree** diffuser data; — — : Reichardt's law; +: exp.

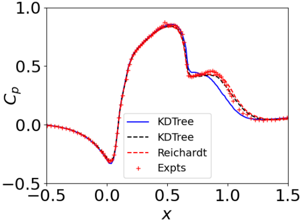

Pressure coefficient.

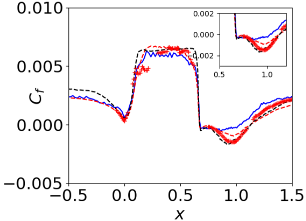

Friction coefficient.

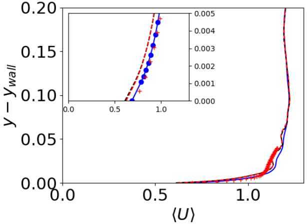

$x = 0.65$.

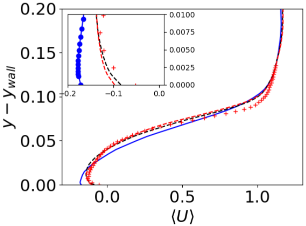

$x = 0.80$.

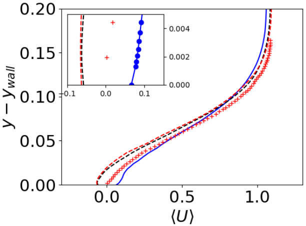

$x = 1.10$.

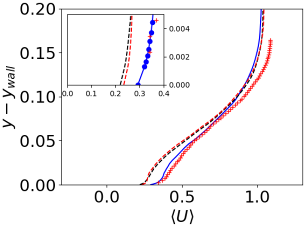

$x = 1.30$.

: **KDTree** hump data; - - - : **KDTree** diffuser data; — — : Reichardt's law; +: exp.

RESULTS, HUMP FLOW. $291 \times 106 \times 16$ CELLS. SHEAR STRESSES

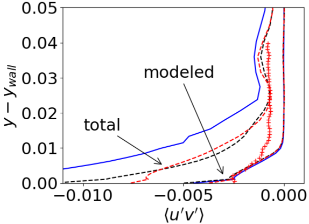

$x = 0.65.$

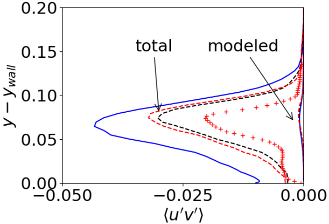

$x = 0.80.$

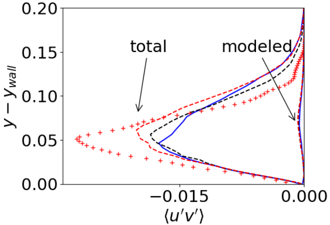

$x = 1.10.$

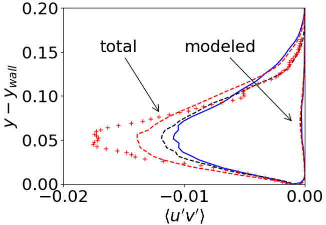

$x = 1.30.$

——— : **KDTree** hump data; - - - : **KDTree** diffuser data; – – : Reichardt's law; +: exp.

Results, Hump Flow. Standard Wall Function mesh, $N_y = 80$

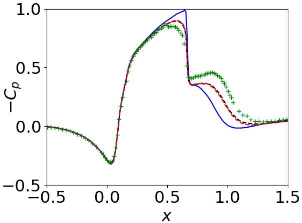

Pressure coefficient.

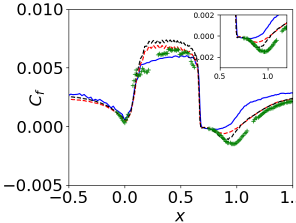

Friction coefficient.

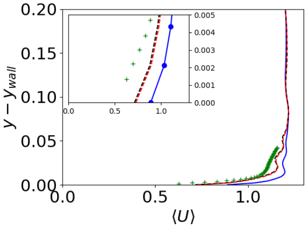

$x = 0.65$.

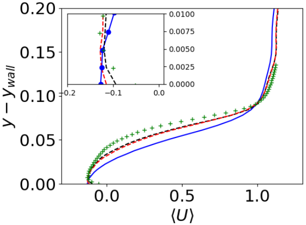

$x = 0.80$.

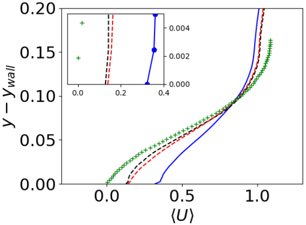

$x = 1.10$.

——— : **KDTree** hump data; - - - : **KDTree** diffuser data; — — : Reichardt's law; +: exp.

URANS/LES INTERFACE.

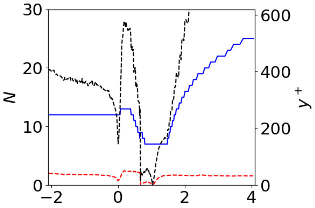

Hump flow.

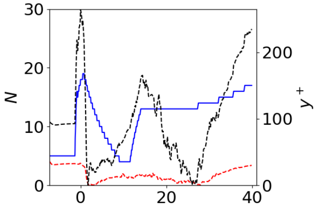

Diffuser flow.

—— : Number of cells in the URANS region (left y axis); – – : y^+ of wall-adjacent cells (right y axis).

- Inlet b.c. taken from a pre-cursor $k-\omega$ simulation at $Re_\theta \simeq 2\,500$
- Grid: $550 \times 90 \times 64$
- Domain: $63 \times 4.6 \times 3.2$.
- Inlet boundary layer thickness: $\delta_{in} = 0.86$
- Inlet k and ε: 2D RANS plus commutation term in k eq. [4, 1].
- Synthetic fluctuations [12, 2] are superimposed on the mean flow

Boundary Layer Flow. Results. 3^{rd} Cell.

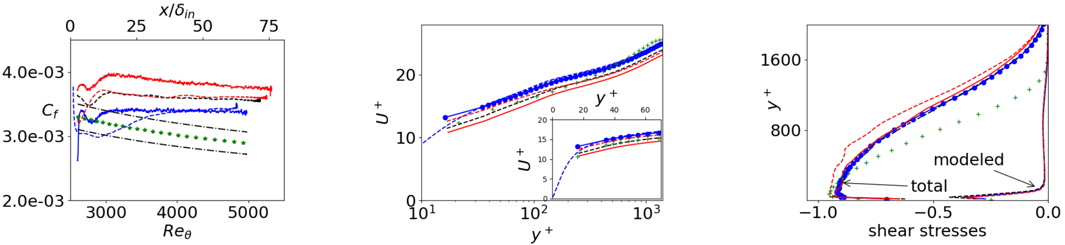

(A) Friction coefficient. (B) Mean velocity. (C) Shear stresses.

u_τ is computed by using U^+ and y^+ at the 4^{th} cell. Velocity and shear stresses are shown at $Re_\theta = 4\,000$. —— : **KDTree** , hump flow - - - : **KDTree** , diffuser flow data, $K = 5$; —— : **KDTree** , diffuser flow data, $K = 1$; – – : Reichardt's wall function; •: cell centers; – – : low-Re IDDES; $*$: $C_f = 2(1/0.384\ln(Re_\theta) + 4.127)^{-2}$; – · – : $\pm 6\%$; +: DNS.

- $Re_\tau = 16\,000$, Inlet-outlet
- Grid: $96 \times 32 \times 32$
- Domain: $9 \times 2 \times 1.6$
- Inlet k and ε: 2D RANS plus commutation term in k eq. [4, 1].
- Synthetic fluctuations [12, 2] are superimposed on the mean flow

Channel Flow. Results.

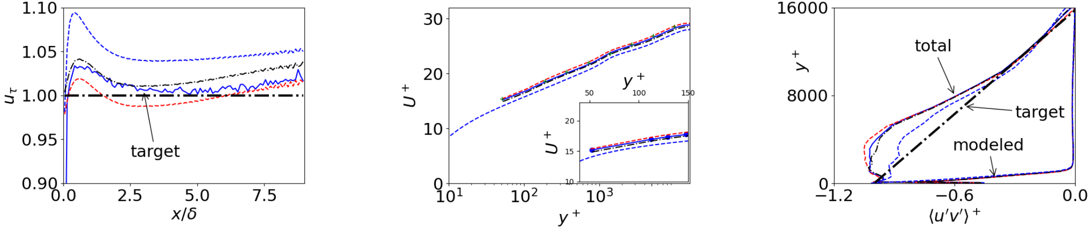

(A) Friction velocity. (B) Mean velocity. (C) Shear stress.

Velocity and shear stress are shown at $x/\delta = 6$. —— : **KDTree** , hump flow - - - : **KDTree** , diffuser flow; – – : low-Re IDDES; —— : **KDTree** , hump flow , $K = 5$; – – : Reichardt's wall function; •: cell centers; +: Reichardt's law

- A new wall function based on **KDTree** (look-up table) has been presented

- A new wall function based on **KDTree** (look-up table) has been presented
  - Two sets of target data are evaluated: diffuser flow ($\alpha = 15^o$) and hump flow.

- A new wall function based on **KDTree** (look-up table) has been presented
  - Two sets of target data are evaluated: diffuser flow ($\alpha = 15^o$) and hump flow.
  - Four flows are usee as test cases: diffuser flow ($\alpha = 15^o$ and $\alpha + 10^o$), hump flow, boundary layer flow and channel flow

- A new wall function based on **KDTree** (look-up table) has been presented
  - Two sets of target data are evaluated: diffuser flow ($\alpha = 15^o$) and hump flow.
  - Four flows are usee as test cases: diffuser flow ($\alpha = 15^o$ and $\alpha + 10^o$), hump flow, boundary layer flow and channel flow
- The diffuser target data set gives in general better results: it's a much simpler, cleaner flow than the hump flow

CONCLUSIONS

- A new wall function based on **KDTree** (look-up table) has been presented
  - Two sets of target data are evaluated: diffuser flow ($\alpha = 15^o$) and hump flow.
  - Four flows are usee as test cases: diffuser flow ($\alpha = 15^o$ and $\alpha + 10^o$), hump flow, boundary layer flow and channel flow
- The diffuser target data set gives in general better results: it's a much simpler, cleaner flow than the hump flow
- Much more target data (many more *x* profiles) are needed in the hump flow than in the diffuser flow

CONCLUSIONS

- A new wall function based on **KDTree** (look-up table) has been presented
  - Two sets of target data are evaluated: diffuser flow ($\alpha = 15^o$) and hump flow.
  - Four flows are usee as test cases: diffuser flow ($\alpha = 15^o$ and $\alpha + 10^o$), hump flow, boundary layer flow and channel flow
- The diffuser target data set gives in general better results: it's a much simpler, cleaner flow than the hump flow
- Much more target data (many more *x* profiles) are needed in the hump flow than in the diffuser flow
- You can downlload Python scripts here

References

[1] S. Arvidson, L. Davidson, and S.-H. Peng. Interface methods for grey-area mitigation in turbulence-resolving hybrid RANS-LES. *International Journal of Heat and Fluid Flow*, 73:236–257, 2018.

[2] M. Carlsson, L. Davidson, S.-H. Peng, and S. Arvidson. Investigation of turbulence injection methods in large eddy simulation using a compressible flow solver. In *AIAA Science and Technology Forum and Exposition, AIAA SciTech Forum*, 2022.

[3] L. Davidson. Zonal PANS: evaluation of different treatments of the RANS-LES interface. *Journal of Turbulence*, 17(3):274–307, 2016.

[4] L. Davidson. Two-equation hybrid RANS-LES models: A novel way to treat k and ω at inlets and at embedded interfaces. *Journal of Turbulence*, 18(4):291–315, 2017.

[5] L. Davidson. pyCALC-LES: a Python code for DNS, LES and Hybrid LES-RANS. Division of Fluid Dynamics, Dept. of Mechanics and Maritime Sciences, Chalmers University of Technology, Gothenburg, 2021.

[6] L. Davidson. Using machine learning for formulating new wall functions for Detached Eddy Simulation. In *14th International ERCOFTAC Symposium on Engineering Turbulence Modelling and Measurements (ETMM14), Barcelona/Digital, Spain 6–8 September*, 2023.

[7] D. Greenblatt, K. B. Paschal, C.-S. Yao, and J. Harris. A separation control CFD validation test case Part 1: Zero efflux oscillatory blowing. AIAA-2005-0485, 2005.

[8] D. Greenblatt, K. B. Paschal, C.-S. Yao, J. Harris, N. W. Schaeffler, and A. E. Washburn. A separation control CFD validation test case. Part 1: Baseline & steady suction. AIAA-2004-2220, 2004.

[9] Andreas Lindholm, Niklas Wahlström, Fredrik Lindsten, and Thomas Schön. *Machine Learning: A First Course for Engineers and Scientists*. Cambridge University Press, 2022.

[10] Menneni Rachana, Jegadeesan Ramalingam, Gajula Ramana, Adigoppula Tejaswi, Sagar Mamidala, and G Srikanth. Fraud detection of credit card using machine learning. *GIS-Zeitschrift für Geoinformatik*, 8:1421–1436, 10 2021.

[11] Sudarshana S Rao and Santosh R Desai. Machine learning based traffic light detection and ir sensor based proximity sensing for autonomous cars. In *Proceedings of the International Conference on IoT Based Control Networks & Intelligent Systems – ICICNIS*, 2021.

[12] M. Shur, P.R. Spalart, M.K. Strelets, and A.K. Travin. Synthetic turbulence generators for RANS-LES interfaces in zonal simulations of aerodynamic and aeroacoustic problems. *Flow, Turbulence and Combustion*, 93:69–92, 2014.

[13] J.A. Sillero, J. Jimenez, and R.D. Moser. One-point statistics for turbulent wall-bounded flows at Reynolds numbers up to $\delta^+ \simeq 2000$. *Physics of Fluids*, 25(105102), 2014.